DOI: 10.1002/chem.201000397

WO_3/TiO_2 Nanotubes with Strongly Enhanced Photocatalytic Activity

Indhumati Paramasivam, Yoon-Chae Nah, Chittaranjan Das, Nabeen K. Shrestha, and Patrik Schmuki*[a]

Initiated by the work of Fujishima and Honda in 1972, over the past decades, the use of particulate or colloidal semiconductors in solutions has extensively been studied for the photocatalytic oxidation of organic waste and pollutants in water.[1–3] By far the most studied material is TiO_2, as it is considered to represent the most suitable photocatalyst, in view of effectiveness and stability against photodecomposition.[4–7] Typically these photocatalytic systems are used in form of nanoparticles, either freely suspended in solution or compacted to a robust photoelectrode. Earlier studies mainly focused on geometric parameters of the particles that influence the photocatalytic activity, such as surface area, size distribution in solution, as well as the TiO_2 crystal structure, which was found to play a crucial role.[8–10] Later, various approaches were reported to enhance the photocatalytic activity of TiO_2, for example, by decorating the surface of TiO_2 nanoparticles with noble metals such as Pt, Pd, Ag, Au, and so forth.[11–15] More recently, improved photocatalytic activity was reached by modifying TiO_2 particles with other oxides (such as Cr_xO_y, Fe_xO_y, V_xO_y, MoO_x, WO_x, etc.).[16–22] The effect of noble particle decoration was mainly interpreted in terms of a facilitated contribution of the photoexcited electrons in the photocatalytic reaction producing, for example, superoxide from O_2 dissolved in aqueous electrolytes, while decoration with other oxides particles may influence the rate of charge transfer to the environment via surface states or junction formation. In general, two main reactions are considered to be relevant for the photocatalytic activity of TiO_2: 1) the generation of valence-band holes that upon ejection to the environment (electrolyte) have an oxidative power sufficient to oxidize almost any organic material and 2) conduction-band electrons ejected to the electrolyte that may form reactive superoxides.[7]

Most recently, advanced geometries of TiO_2 have been increasingly explored, in particular self-ordered TiO_2 nanotubes (TiNT) have attracted wide attention due to the high level of geometrical definition combined with a high surface area (for an overview see references [23–26]). Such self-ordered TiO_2 nanotubular layers can easily be grown on Ti metal sheets by a simple but optimized electrochemical anodization in F^- containing electrolytes.[23,24,27,28] Investigations of their photocatalytic properties have shown that these tubular layers can be more efficient than classical nanoparticulate layers of a comparable thickness.[29,39–41] Self-ordered oxide nanotubes cannot only be grown on pure Ti, but also on other transition metals such as Mo, W, Ta, Nb, and so forth, and a full range of Ti alloys including TiW, TiNb, TiAl, TiMo, TiTa.[30–34] In the present work, we demonstrate a very strong effect of tungsten addition to the TiO_2 nanotubes in terms of their photocatalytic activity. For this, different TiW alloys (Ti 0.2 at % W (Ti 0.2 W) and Ti 9 at % W (Ti 9 W)) as well as pure Ti were anodized to form $\approx$2 μm-long self-organized tube layers as shown in Figure 1. To achieve these self-organized layers different anodization conditions had to be applied as outlined in the Supporting Information. For all cases, comparable dimensions of nanotubular layers with a tube length between $\approx$2.2 μm to 2.6 μm and a diameter (obtained from SEM cross sections) between $\approx$85 nm to 100 nm were used. For the TiW alloys (Figure 1a–d), a thin porous initiation layer is present on the top of the highly ordered nanotubes, as visible in the cross-sectional images of Figure 1b and d. Figure 1e and f show for comparison, the top view and cross section of pure TiO_2 nanotube layers. The top layer can be removed,[35] but this was found to not affect the results strongly.

[a] I. Paramasivam, Y.-C. Nah, C. Das, N. K. Shrestha, Prof. Dr. P. Schmuki
Department of Materials Science WW-4
Institute of Corrosion and Surface Science (LKO)
University of Erlangen—Nürnberg
Martensstr.7, 91058 Erlangen (Germany)
Fax: (+49) 9131-852-7575
E-mail: schmuki@ww.uni-erlangen.de

Supporting information for this article is available on the WWW under http://dx.doi.org/10.1002/chem.201000397. It contains experimental descriptions, XRD patterns of TiO_2-WO_3 nanotubes at 350 °C and 550 °C, and EDX of elemental compositions for Ti 9 W and Ti 0.2 W.

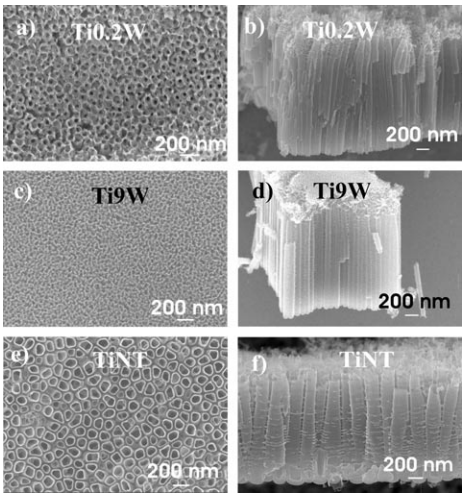

Figure 1. Scanning electron micrographs of top view (left) and cross section (right) of self-organized nanotube layers formed on Ti0.2W(a,b); Ti9W (c,d) and Ti (e,f).

After formation, all the tube layers are amorphous, but they can be converted to a crystalline structure by thermal annealing. Figure 2 shows the XRD patterns for the nanotube layers of Figure 1 after the samples were annealed in air at 450 °C for 1 h.

The results indicate that pure TiNT samples underwent, after annealing, a transformation from amorphous to a mainly anatase structure together with slight traces of rutile. For the oxide layers formed on the alloys, the presence of WO_3 in the oxide is apparent from the XRD peak at 23.1° corresponding to a monoclinic phase. As expected this peak is significantly more apparent for nanotube layers formed on the 9 at% W alloy than for the oxide formed at 0.2 at% W. XRD data for different annealing conditions are given in the Supporting Information. EDX and XPS (shown in Supporting Information) showed that the composition of the tube oxides corresponds to the substrate, that is, for the Ti9W alloy tungsten content in the oxide was $\approx$10 atomic%, whereas in case of Ti0.2W no significant W peak is visible in XRD as this content is below the detection limit. Moreover, surface chemical composition and the oxidation states of Ti and $TiWO_x$ nanotubes were characterized by X-ray photoelectron spectroscopy (XPS) as shown in Figure S3 in the Supporting Information. The position of binding energies (BE) of W4 $f_{7/2}$ and W4 $f_{5/2}$ peaks is slightly shifted towards lower energy from 35.1 and 37.3 eV to 36.8 and 34.6 eV respectively. This difference in binding energy $\Delta BE = 0.5$ eV, when compared with reference oxide,[32] implies that WO_3 is substoichiometric or has oxygen vacancies thus forming WO_{3-x}.

The photocatalytic activity for the different WO_3 contents was then investigated by decomposition measurements of an organic dye (Rhodamine B, RhB). Figure 3a shows the degradation kinetics of RhB for samples with different contents of W (0.2 at% and 9 at%) and for pure TiNTs after annealing at 450 °C. No detectable degradation of RhB dye (photofading) was observed in absence of catalyst, that is, upon plain UV ($\lambda = 325$ nm) illumination. The linear profile indicates that the decomposition kinetics can be approximated by a first-order rate law.[36] Pseudo-first-order rate constants (k) were thus determined from the relation: $\ln(C/C_0) = k\tau$, in which τ is the time of irradiation. The highest photocatalytic activity is clearly observed with 0.2 at% of W ($k = 2.09\ h^{-1}$), followed by 9 at% of W ($k = 1.31\ h^{-1}$) and the non-doped TiNT ($k = 0.68\ h^{-1}$). Therefore, the influence of the annealing temperature for low-content TiW samples was further investigated as shown in Figure 3b. Clearly, for all temperatures, W doping showed a beneficial effect on the photocatalytic properties of the TiNTs. The rate constants for this annealing series were determined as: $k_{450\,°C} = 2.09\ h^{-1} > k_{550\,°C} = 1.39\ h^{-1} > k_{350\,°C} = 1.21\ h^{-1}$. From the XRD

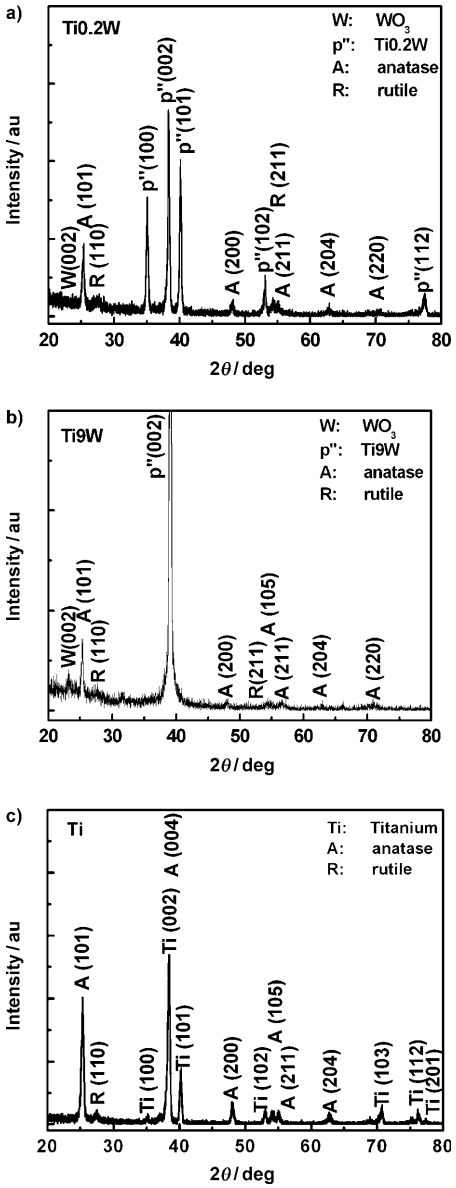

Figure 2. X-ray diffraction patterns for the layers of Figure 1 after annealing at 450°.

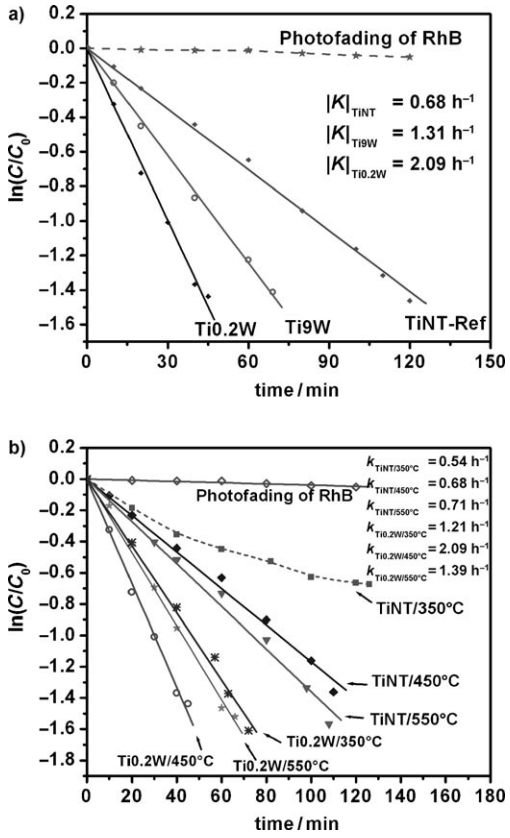

Figure 3. Photocatalytic degradation of Rhodamine B (RhB, $C_0 = 20\ \mu M$ in aqueous solution) under UV light ($\lambda = 325$ nm). a) Comparison of W-doped and undoped TiO_2 nanotubes. b) Effect of annealing on W-doped and undoped TiO_2 nanotubes.

spectra in the Supporting Information it is clear that at 350 °C the crystallization of WO_3 is not entirely complete. On the other hand, at 550 °C significant amount of rutile has been formed in the nanotube wall. Rutile is generally much less active in photoelectrochemical applications due to a significantly lower electron mobility.[29]

To explore the beneficial effect of WO_3 and the maximum activity for low WO_3 contents in the nanotubular system, a series of photoelectrochemical experiments was performed. From Figure S4 in the Supporting Information, it is evident that a main effect of WO_3 addition is, as expected, a lowering of the optical band gap from 3.12 eV for the anatase tubes to 3.08 eV for Ti0.2W and 2.98 eV for Ti9W material; that is, the effect is the largest for the higher W content. When performing photocatalytic measurements under constant band-bending conditions (fixed applied potential) and exciting only the visible spectral part as shown in Figure 4a, the nanotube layer containing only 0.2 at% W still shows the highest efficiency. In other words, neither different band-bending nor the altered visible absorption coefficient can be the reason for the maximum efficiency at 0.2 at% W content.

If we additionally considers the photocurrent results of Figure 4b and c, we observe slower photocurrent transient kinetics for the highest W content and most drastic increase

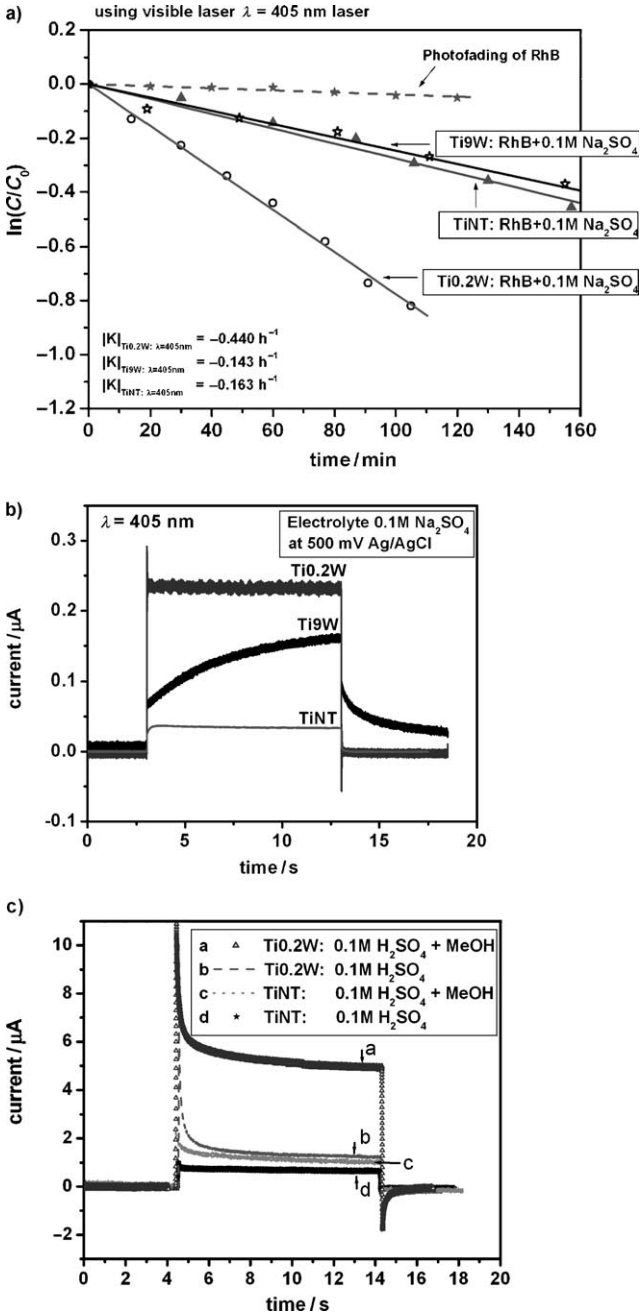

Figure 4. Photocatalytic degradation of Rhodamine B (RhB, $C_0 = 20\ \mu M$ in aqueous solution) under visible light $\lambda = 405$ nm. a) Comparison of W-doped and undoped TiO_2 nanotubes. Photocurrent transient spectra with voltage bias of 500 mV Ag/AgCl in b) 0.1 M Na_2SO_4 electrolyte and c) in 0.1 M H_2SO_4 with and without 2 M methanol addition.

of the photoresponse if a hole capture agent (CH_3OH) is added to the electrolyte. From these results one may ascribe the strongly beneficial effect of WO_3 to the photocatalytic activity mainly to an enhanced hole-transfer kinetics to the electrolyte, while at the same time the detrimental effect of a too high WO_3 content may originate from charge trapping effects in the bulk. This is in line with literature,[36,39] which suggests the presence of WO_3 in TiO_2 to influence the re-

combination rate of the photoproduced electron–hole (e^-–h^+) pairs that may be either due to localized heterojunction formation[38] (due to mismatch of the TiO_2 and WO_3 band energies) or to the formation of activating surface species such as W^{VI} states. The present work clearly favors the formation of specific surface features such as W^{VI} states that act as mediators for charge transfer to the electrolyte.

Overall, to emphasize the drastic increase obtained by WO_3 doping of TiO_2 nanotubes, we compare in Figure 5 the

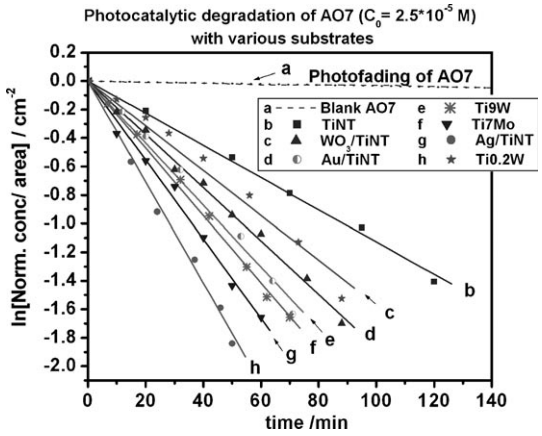

Figure 5. Photocatalytic degradation of AO7 ($C_0 = 2.5 \times 10^{-5}$ M in aqueous solution) under UV light ($\lambda = 325$ nm). Comparison of various TiO_2 nanotubes that were modified with Ag, Au, WO_3 nanoparticles, and various mixed oxide nanotubes against undoped TiO_2 nanotubes are shown.

photocatalytic activity to different approaches to increase the photocatalytic activity of TiO_2 nanotubes, such as metal decoration (Ag/TiNT, Au/TiNT[40]), metal oxide decoration (WO_3/TiNT), and using other mixed oxide nanotubes (Ti7Mo[42]). Clearly, the low WO_3-content TiO_2 nanotubes investigated in the present work shows the most superior enhancement of all investigated strategies investigated up to now.

In summary, the present work shows a strongly beneficial effect of WO_3 addition for the photocatalytic activity of TiO_2 nanotube layers both in UV and the visible region. Remarkable is that the strongest enhancement of the photocatalytic activity is observed for the addition of low WO_3 content (0.2 at% W) to the Ti nanotubes. This is ascribed to a facilitated charge transfer for the WO_3-containing material. Overall, the findings presented here provide not only the basis for enhanced environmental photocatalysis, but also for other applications of TiO_2 nanotubes such as surface wetting,[43] antifogging, or regarding payload-release properties.[44]

Experimental Section

Anodic growth of nanotubes layers: TiO_2 nanotubes were grown by anodization of a Ti foil at 30 V for 3 h[40,41] in a mixture of glycerol (1, 2, 3-propanetriol), water (60:40 vol%) and 0.27 M NH_4F. For Ti0.2W and Ti9W, the anodization was carried out at 120 V for 45 min and 60 min, respectively, in a solution of ethylene glycol with 0.2 M HF after aging the solution for 24 h.[32]

Annealing: Thermal treatment was carried out in air by using a rapid thermal annealer (Jipelec JetFirst) at 450 °C for 1 h with heating and cooling rate of 30 °C min^{-1}.

Photocatalytic activity:The photocatalytic activites of TiNTs and W-doped TiNTs were evaluated by measuring the photodegradation of Rhodamine B (RhB) dye in aqueous solution (initial concentration $C_0 =$ 20 μM) using a UV/Vis spectrometer (Lambda XLS +, Perkin–Elmer). Every sample was prepared with same area of 1.35 cm^2, which was immersed in a quartz couvette containing RhB (2.5 mL, $C_{28}H_{31}N_2O_3Cl$, $C_{initial} = 20$ μM) and kept for 30 min in dark (in dye) to establish the dye adsorption/desorption equilibrium. Certain experiments (as shown in Figure 5, of Acid Orange 7 (AO7, 3 mL, $C_{16}H_{11}N_2O_4SNa$, $C_{initial} = 2.5 \times 10^{-5}$ mol L^{-1}) a model pollutant was also used as a standard dye for degradation. Once the equilibrium was established, a UV laser (He-Cd, Kimmon Japan $\lambda = 325$ nm, $I_{light} = 60$ mW cm^{-2}) and visible laser of $\lambda =$ 405 nm was used for irradiation of the sample surface. The solution in the couvette was stirred at 300 rpm. Experiments were done at room temperature. The maximum absorbance of RhB dye was observed at $\lambda =$ 554 nm. Therefore, change in concentration is recorded at regular intervals of time (of approx. every 20 min) at this wavelength.

Photocurrent transient measurements: To investigate the photoresponse of TiNT, Ti0.2W and Ti9W layers, photoelectrochemical measurements were carried out in an aqueous solution of 0.1 M H_2SO_4. Photocurrent spectra and transients were recorded at a constant potential of 500 mV versus Ag/AgCl in the illumination range of 320–600 nm using an Oriel 6356 Xe lamp and an Oriel Cornerstone 7400 1/8 m monochromator.

SEM: A field emission scanning electron microscope (HITACHI SEM FE S4800) was used to investigate morphology of samples.

EDX: Semiquantitative analysis of nanotubes layer were performed by energy dispersive X-ray spectroscopy (EDX). The contents of WO_3 are 10.73 and 5.6 at% W outside and inside the anodized area respectively.

XRD: X-ray diffraction (XRD) analysis was performed Philips X'Pert PRO diffractometer with monochromatic $Cu_{K\alpha}$ radiation.

Acknowledgements

We greatly acknowledge the Deutsche Forschungsgemeinschaft (DFG), Cluster of Excellence, Engineering of Advanced Materials EAM (Area-Catalysis D5) in Friedrich-Alexander University, Erlangen for funding. Dr. M. Oehring (GKSS Forschungszentrum in Geesthacht) is also gratefully acknowledged for providing the Ti W alloys. N. K. Shrestha acknowledges the Humboldt foundation for his funding.

Keywords: electrochemistry · nanostructures · photocatalysis · titanium · tungsten

[1] T. Kawai, T. Sakata, *Nature* **1980**, *286*, 474.
[2] C. K. Grätzel, M. Jiransek, M. Grätzel, *J. Mol. Catal.* **1987**, *39*, 347.
[3] A. L. Pruden, D. F. Ollis, *J. Catal.* **1983**, *82*, 404.
[4] R. W. Matthews, *J. Catal.* **1988**, *111*, 264.
[5] M. Barbeni, A. E. Pramauro, E. Pellizetti, *Chemosphere* **1985**, *14*, 195.
[6] T. Inoue, A. Fujishima, S. Konishi, K. Honda, *Nature* **1979**, *277*, 637.
[7] H. Gerischer, A. Heller, *J. Phys. Chem.* **1991**, *95*, 5261.
[8] A. H. Harada, T. Ueda, *Chem. Phys. Lett.* **1984**, *106*, 229.
[9] H. V. Damme, E. N. Serpone, E. Pelizzetti, *Photocatalysis—Fundamentals and Applications*, Wiley, New York, **1989**.
[10] R. I. Bickley, T. Gonzalez-Carreno, J. S. Lees, L. Palmisano, R. J. D. Tilley, *J. Solid State Chem.* **1991**, *92*, 178.

[11] J. Papp, H. S. Shen, R. Kershaw, A. K. Dwight, A. Wold, *Chem. Mater.* **1993**, *5*, 284.
[12] C. M. Wang, A. Heller, H. Gerischer, *J. Am. Chem. Soc.* **1992**, *114*, 5230.
[13] W. Choi, A. Termin, M. R. Hoffmann, *J. Phys. Chem.* **1994**, *98*, 13669.
[14] M. Anpo, S. Dohshi, M. Kitano, Y. Hu, M. Takeuchi, M. Matsuoka, *Annu. Rev. Mater. Res.* **2005**, *35*, 1.
[15] A. Sclafani, J. M. Herrmann, *J. Photochem. Photobiol. A* **1998**, *113*, 181.
[16] K. Nagaveni, M. S. Hedge, G. Madras, *J. Phys. Chem. B* **2004**, *108*, 20204.
[17] C. Martin, I. Martin, V. Rives, L. Palmisano, M. Schiavello, *J. Catal.* **1992**, *134*, 434.
[18] L. Palmisano, V. Augugliaro, A. Sclafani, M. Schiavello, *J. Phys. Chem.* **1988**, *92*, 6710.
[19] Y. Yang, X.-J. Li, J.-T. Chen, L.-Y. Wang, *J. Photochem. Photobiol. A* **2004**, *163*, 517.
[20] M. W. Xiao, L. Wang, X. Huang, Z. Dang, *J. Alloys Compd.* **2009**, *470*, 486.
[21] L. Gomathi Devi, B. N. Murthy, *Catal. Lett.* **2008**, *125*, 320.
[22] Y. R. Do, W. Lee, K. Dwight, A. Wold, *J. Solid State Chem.* **1994**, *108*, 198.
[23] J. M. Macak, H. Tsuchiya, A. Ghicov, K. Yasuda, R. Hahn, S. Bauer, P. Schmuki, *Curr. Opin. Solid State Mater. Sci.* **2007**, *11*, 3.
[24] A. Ghicov, P. Schmuki, *Chem. Commun.* **2009**, 2791.
[25] Y. C.-Nah, I. Paramasivam, P. Schmuki, *ChemPhysChem* **2010**, **accepted**.
[26] P. Roy, D. Kim, H. Lee, P. Schmuki, *Nanoscale* **2010**, *2*, 45.
[27] V. Zwilling, E. Darque-Ceretti, *Electrochim. Acta* **1999**, *45*, 921.
[28] J. M. Macak, H. Tsuchiya, P. Schmuki, *Angew. Chem.* **2005**, *117*, 7629; *Angew. Chem. Int. Ed.* **2005**, *44*, 7463.
[29] J. M. Macák, M. Zlamal, J. Krysa, P. Schmuki, *Small* **2007**, *3*, 300.
[30] S. Berger, H. Tsuchiya, P. Schmuki, *Chem. Mater.* **2008**, *20*, 3245.
[31] A. Ghicov, S. Aldabergenova, H. Tsuchyia, P. Schmuki, *Angew. Chem.* **2006**, *118*, 7150; *Angew. Chem. Int. Ed.* **2006**, *45*, 6993.
[32] Y.-C. Nah, A. Ghicov, D. Kim, S. Berger, P. Schmuki, *J. Am. Chem. Soc.* **2008**, *130*, 16154.
[33] N. K. Shrestha, Y.-C. Nah, H. Tsuchiya, P. Schmuki, *Chem. Commun.* **2009**, 2008.
[34] W. Wei, S. Berger, N. K. Shrestha, P. Schmuki, unpublished results,.
[35] Y. C. Nah, N. K. Shrestha, D. Kim, S. P. Albu, I. Paramasivam, P. Schmuki, *Electrochem. Solid-State Lett.* **2010**, *13*, K73.
[36] M. Zlamal, J. M. Macak, P. Schmuki, J. Krysa, *Electrochem. Commun.* **2007** *9*, 2822.
[37] A. Di Paola, G. Marci, L. Palmisano, M. Schiavello, K. Uosaki, S. Ikeda, B. Ohtani, *J. Phys. Chem. B* **2002**, *106*, 637.
[38] G. Marcì, L. Palmisano, A. Sclafani, A. M. Venezia, R. Campostrini, G. Carturan, V. R. C. Martin, G. Solana, *J. Chem. Soc. Faraday Trans.* **1996**, *92*, 819.
[39] T. L. Thompson, J. T. Yates, *J. Phys. Chem. B* **2005**, *109*, 18230.
[40] I. Paramasivam, J. M. Macak, P. Schmuki, *Electrochem. Commun.* **2008**, *10*, 71.
[41] I Paramasivam, A Avhale, A Inayat, A Bösmann, P Schmuki, W Schwieger, *Nanotechnology* **2009**, *20*, 225607.
[42] P. Agarwal, I. Paramasivam, N. K. Shrestha, P. Schmuki, *Chem. Asian J.* **2010**, *5*, 66.
[43] E. Balaur, J. M. Macak, H. Tsuchiya and P. Schmuki, *J. Mater. Chem.* **2005**, *15*, 4488.
[44] a) Y.-Y. Song, F. Schmidt-Stein, S. Bauer, P. Schmuki, *J. Am. Chem. Soc.* **2009**, *131*, 4230; b) Y.-Y. Song, H. Hildebrand, P. Schmuki, *Electrochem. Commun.* **2009**, *11*, 1429; c) Y.-Y. Song, P. Roy, I. Paramasivam, P. Schmuki, *Angew. Chem.* **2010**, *49*, 351; *Angew. Chem. Int. Ed.* **2010**, *122*, 361; d) F. Schmidt-Stein, R. Hahn, J.-F. Gnichwitz, Y.-Y. Song, N. K. Shrestha, A. Hirsch, P. Schmuki, *Electrochem. Commun.* **2009**, *11*, 2077.

Received: February 14, 2010
Published online: July 19, 2010

